Lysine harvesting gives rise to an underground polyamine pathway and is a new cellular antioxidant strategy

Viridiana Olin-Sandoval[1,4], Jason Shu Lim Yu[2], Leonor Miller-Fleming[1,8], Mohammad Tauqeer Alam[5], Stephan Kamrad[2], Clara Correia-Melo[2], Robert Haas[1,2], Joanna Segal[2], David Alejandro Peña Navarro[9], Carmen Lucia Herrera[2], Oscar Méndez-Lucio[7] , Jakob Vowinckel[1,6] Michael Mülleder[1,2,3], and Markus Ralser[1,2,3*]

1. Department of Biochemistry, University of Cambridge, Cambridge, United Kingdom
2. The Molecular Biology of Metabolism Laboratory, The Francis Crick Institute, London, United Kingdom
3. Department of Biochemistry, Charité University Medicine, Berlin, Germany
4. Present address: Department of Nutrition Physiology, Instituto Nacional de Ciencias Medicas y Nutricion Salvador Zubiran, Mexico City, Mexico
5. Warwick Medical School, University of Warwick, Warwick, United Kingdom
6. Present address: Biognosys AG, Schlieren, Switzerland
7. Facultad de Quimica, Departamento de Farmacia, Universidad Nacional Autonoma de Mexico, Mexico City, Mexico
8. Present address: Medical Research Council Mitochondrial Biology Unit, University of Cambridge, Cambridge, United Kingdom
9. Department of Biotechnology, BOKU - University of Natural Resources and Life Sciences, Vienna, Austria

Correspondence should be addressed to markus.ralser@crick.ac.uk

Abstract

We report a so far overlooked, but powerful, metabolic mechanism that protects cells in stress situations. A proteomic time course experiment linked the antioxidant role of the yeast polyamine transporter Tpo1 to lysine metabolism. A connection between polyamine and lysine metabolism was established by a promiscuous enzymatic reaction, in which the first enzyme of the polyamine pathway, Spe1p, decarboxylates lysine and forms an alternative polyamine, cadaverine. Enzymology revealed that this reaction can only proceed when lysine reaches very high cellular concentrations. We found that yeast accumulates lysine to reach concentrations that can be seventy to a hundred times higher than the concentrations required for growth and that the polyamine export machinery is important to enable this harvest. Comparable harvesting was not observed for other amino acids. Lysine harvesting was found to increase the concentration of NADPH, that is channelled into the antioxidant system to maintain a much higher glutathione pool, to mitigate ROS levels, and to increase oxidant tolerance. Hence, our results show that nutrient uptake occurs not only to enable cell growth but also to reconfigure metabolism to increase robustness by mounting a new type of metabolic antioxidant protection.

INTRODUCTION

Both single and multicellular organisms depend on anti-stress mechanisms that enable them to deal with sudden changes in the environment, including exposure to heat and oxidants. Key features of this anti-stress machinery include redox signalling and sensing [1], the induction of heat-shock proteins and molecular chaperones [2], the ability to slow growth and halt the cell cycle [3], and an elaborate capacity to repair oxidised macromolecules, as well as the antioxidant function of the glutaredoxin, thioredoxin and peroxiredoxin systems [4,5]. In humans, deficiencies in antioxidant metabolism, as well as oxidative damage on metabolites and macromolecules caused by age, have been associated with cancer, neurodegenerative disorders, and cardiovascular diseases [6–8].

The redox machinery and successful balancing of the cellular redox state depend on metabolism to provide the required cofactors, in particular, NADPH, and on antioxidant metabolites, such as glutathione [9,10]. So far, the glycolysis/pentose phosphate pathway (PPP) transition, which was discovered in yeast [11] and conserved from bacteria to humans, is the best understood metabolic balancing mechanism. Through the concerted action of transcriptional, post-transcriptional and metabolic processes acting at different timescales, PPP activity sharply increases, fulfilling the demand through higher flux within reactions that form NADPH, which in turn serves as an essential cofactor for antioxidant enzymes including the glutaredoxin system [11–19].

Other metabolic mechanisms that support the stress tolerance of cells are less understood. A prominent group of metabolites that have been repeatedly associated with robustness of cells in stress situations are polyamines, specifically putrescine (Put), spermidine (Spd) and spermine (Spm), which are multifunctional polycations found in all organisms (Figure 1a) [20–27]. To date, it is not fully clear how the polyamine pathway participates in promoting stress resistance in the cell, but it is likely that the multi-functional nature of polyamines affects many processes [20]. For instance, polyamines are pH buffers and can act as antioxidants [28]. A largely unexplained role in antioxidant protection is attributed to the polyamine export machinery. When exposed to H_2O_2, yeast cells lacking or overexpressing the polyamine exporter *TPO1* time the induction of several heat-shock proteins improperly, decreasing their oxidant tolerance [29].

In trying to explain the metabolic basis of the oxidant tolerant phenotype of Δ*tpo1* cells, we identified a so far overlooked antioxidant principle. Proteomics revealed that *TPO1* deletion alters lysine metabolism in cells exposed to H_2O_2. We then found that polyamine and lysine catabolism are connected by an alternative polyamine, cadaverine. This is formed via a side-reaction - i.e. through substrate promiscuity - by Spe1p, the yeast ornithine decarboxylase that in its prominent function, catalyses the first reaction of the conventional polyamine pathway. We revealed that the promiscuous activity of Spe1p on lysine achieves relevant rates only when lysine levels are very high. We found that when cells have access to extracellular sources of lysine, they harvest the amino acid to reach

extreme cellular concentrations that greatly exceed the amounts required for cell growth and that functional polyamine export machinery is required to enable this extensive harvest. Lysine harvesting feedback-inhibits lysine biosynthesis and protects the cells by increasing the availability of NADPH and glutathione concentrations. Ultimately, this mechanism decreases ROS levels and increases resistance to extracellular oxidant exposure. Hence, metabolite import into cells occurs not only to fulfil biosynthetic demands for cell growth but also to mount robustness.

RESULTS

Lysine metabolism and polyamine export are linked via promiscuous activity of ornithine decarboxylase

TPO1 is the prime polyamine exporter in *Saccharomyces* [30–32], and its deletion alters the yeast anti-oxidant response in a largely unexplained manner [29]. We analysed proteomic time-course data [29], obtained by SWATH-MS [33], to identify whether specific metabolic processes could be altered in Δ*tpo1* cells and contribute to their oxidant sensitivity. Consistent with oxidant-induced cell cycle arrest [29], the differentially expressed genes were enriched for genes associated with cell proliferation and cell cycle, including nucleic acid biosynthesis, as well as for antioxidant and stress response proteins (Supplementary Figure 2). Unexpectedly, we also obtained a specific signature of enzymes participating in lysine metabolism. These were found to be induced differently in Δ*tpo1* compared to the WT strain upon H_2O_2 treatment. Quantitatively speaking, the changes were moderate (around 4-fold), but several enzymes of the pathway, Lys20p and Lys21p (homocitrate synthases), Aco2p (aconitase), Lys9p (saccharopine dehydrogenase) and Lys12p (homoisocitrate dehyrogenase) (see Supplementary Figure 1 for a pathway map), all showed a consistent pattern and responded faster and more pronounced in the Δ*tpo1* mutant (Figure 1b). As we have recently shown, metabolism is typically regulated by multiple coordinated expression changes acting in concert [34], suggesting an association of polyamine and lysine metabolism upon H_2O_2 exposure.

As the coordinated response in enzyme expression does not necessarily indicate increased activity of a pathway, but can indicate compensation or altered biological function, we continued by dissecting the nature of the association between lysine and polyamine metabolism. A potential link between the two pathways was provided by their chemistry. Decarboxylation of lysine would results in the formation of cadaverine, a close structural analogue of putrescine, the precursor for spermine and spermidine synthesis, all substrates of *TPO1* (Figure 1c). In contrast to bacteria and plants, in which enzymatic lysine decarboxylation has been reported, *Saccharomyces* lacks a *bona fide* lysine decarboxylase [35–38]. However, work done over the last decade has highlighted that the absence of an enzyme is insufficient to prove the absence of a reaction, as promiscuous and non-

enzymatic reactions significantly contribute to the metabolome [39]. We established a liquid-chromatography selective reaction monitoring (LC-SRM) assay, and quantified cadaverine in yeast cultures grown in the presence or absence of physiological lysine concentrations (25 μg/mL). Only trace amounts of cadaverine (0.26 ± 0.052 pmol/OD_{600nm}) were detected in yeast grown in synthetic minimal media (SM), but in the presence of lysine, the levels increased 22 times (Figure 1d). A potential candidate for this reaction was ornithine decarboxylase (Spe1p, YKL184W). As ornithine is structurally analogous to lysine, we considered it possible that this enzyme might accept lysine as a promiscuous substrate (Figure 1a and c). Although Δ*spe1* cells still contained trace amounts of cadaverine (Figure 1d), any increase in cadaverine levels upon lysine supplementation was eliminated by the Δ*spe1* deletion (Figure 1d). We subsequently performed an isotope tracer experiment, and incubated WT and Δ*spe1* cells with or without $^{13}C_6{}^{15}N_2$-lysine. In WT cells, $^{13}C_5{}^{15}N_2$-cadaverine was formed at high levels. However, in Δ*spe1* cells, none of the tracer was converted into $^{13}C_5{}^{15}N_2$-cadaverine (Figure 1e), confirming that Spe1p was the enzyme responsible for lysine to cadaverine decarboxylation. The pathway level provided further confirmation that cadaverine formation occurs as part of the canonical polyamine pathway. Firstly, we detected decreased cadaverine concentrations in Δ*spe2* (deleted for S-adenosylmethionine decarboxylase (AdoMetDC)), Δ*spe3* (spermidine synthase) and Δ*spe4* (spermine synthase) knockout strains, in which the canonical pathway is feedback-inhibited as a consequence of media supplementation that compensates for polyamine auxotrophy [40] (Figure 1d). Vice versa, cadaverine biosynthesis did not decrease the concentrations of spermidine and spermine, but promoted an increase in putrescine (Supplementary Figure 3).

To gain insights into the mechanisms, we continued with molecular docking calculations and obtained a Spe1p (UniProt ID: P08432 [41]) 3D structure by homology modelling, using the crystal structure of ornithine decarboxylase from *Leishmania donovani* (PDB ID: 2OO0[42]) as a template. This analysis revealed that, due to their highly similar structure, both ornithine and lysine can bind to the catalytic site of Spe1p (Figure 1f). Both compounds are stabilised by hydrogen bonding between the amino group in the ligand with Asp363 and Tyr354 along with a structural water molecule. The calculations indicated that Spe1p should have a much higher affinity for ornithine than for lysine, explained by the slightly different size of the ligands. Although lysine fits in the binding site, it needs to overcome steric hindrance in order to share the catalytic site with the cofactor, pyridoxal phosphate. On the other hand, ornithine, which has one carbon less in the aliphatic chain, appears to fit well together with the cofactor in the catalytic site of Spe1p.

To test these predictions, we expressed and purified Spe1p recombinantly, and analysed its catalytic properties by establishing a mass-spectrometry based *in vitro* enzymatic assay (Table 1). We found that Spe1p can indeed decarboxylate both ornithine and lysine and form putrescine and cadaverine, respectively (Figure 1g and 1h).

Confirming the molecular docking analysis, the affinity and the catalytic efficiency of Spe1p for ornithine is much higher than for lysine. Indeed the *in vitro Km* for lysine decarboxylation is only in the millimolar range (Figure 1g and 1h, Table 1). Despite this low affinity for lysine, Spe1p produced considerable amounts of cadaverine, indicating that this amino acid must have been present at an extremely high concentration.

Yeast cells harvest extensive amounts of lysine

Yeast cells are prototrophic for lysine. The biosynthetic capacity is however fully sufficient to promote cell growth; supplementing lysine to minimal media did not accelerate growth (Supplementary Figure 4). Under these conditions we measured an intracellular lysine concentration of 4.93 ± 1.82 nmol per OD_{600nm}. Assuming a cell volume of 45.54 fL and a concentration of 3.2 x 10^7 cells/OD_{600nm} for the strain BY4741 grown in SM [43], this would correspond to approximately 3.01 ± 1.12 mM in average intracellular concentration, a concentration range similar to what has been previously reported [43]. However, in the presence of physiological amounts of lysine (25 μg/mL), we observed a remarkable 71.2 fold increase to 322.75 nmol per OD_{600nm}, corresponding to an estimated cellular concentration of 215.2 mM (Figure 2a, Table 1). Upon deletion of *TPO1,* this harvesting of extracellular lysine was impaired. Lysine levels accumulated to only half the concentration measured in WT cells (42.5 times of the minimal media levels) (Figure 2a), corresponding to an estimated value of 104.2 mM, which is 30 times the normal cellular levels of lysine. Hence, wild-type cells harvest large amounts of lysine. To further gauge the specificity of lysine accumulation, we measured the intracellular concentration of all other proteinogenic amino acids. Both when each amino acid was supplemented individually or all amino acids as part of yeast extract, extensive harvesting was only observed for lysine, up to hundred-times higher as the concentration when cells self-synthesize lysine (Figure 2b). Thus, in the presence of extracellular amino acids, cells specifically import lysine to reach very high intracellular concentrations of this amino acid.

Lysine harvesting reprograms NADPH metabolism and increases oxidant resistance

High product concentrations inhibit enzymatic reactions [44] and indeed, feedback inhibition of the lysine biosynthetic pathway in the presence of lysine has been reported previously [42–45]. To test how effectively this feedback inhibition occurs in lysine harvesters, we measured lysine uptake rates during growth of prototrophic and auxotrophic BY4742 (Δ*lys2*) strains in SM supplemented with lysine (SM+Lys (25 μg/mL)), as well as in synthetic complete media (SC) that contains lysine among other amino acids. In both conditions, the lysine prototrophs consumed lysine at a similar rate as the auxotrophs, despite only the latter relying on the extracellular pool for growth (Figure 2c). Hence, in the presence of extracellular lysine, cells fully switched from lysine self-synthesis to lysine consumption.

To picture the metabolic changes induced by this reprogramming, we used a genome-scale metabolic modelling approach and performed flux balance analysis (FBA). We expanded a manually curated metabolic network reconstruction [45] by adding the lysine decarboxylation reactions and four reactions for transporting and exchanging cadaverine and aminopropylcadaverine (APC) (Figure 3a). The naive model (optimal growth-specific) predicted that lysine harvesting would induce a system wide change in NADPH forming reactions, reflecting that, when cells harvest lysine, less NADPH is required for growth (Supplementary Figure 5). Optimized for growth, the naive model consequently predicted that cells would reduce the flux in NADPH producing pathways, of which the oxidative branch of the pentose phosphate pathway is the main source (Supplementary Figure 5). A second biological possibility was however that rather than diminishing NADPH production, cells could also channel the molecule into other metabolic processes, of which the glutaredoxin system is a major sink. We exploited phenotypic assays to test in which direction NADPH availability changes in cells that harvest lysine. Cells lacking glucose 6-phosphate dehydrogenase (Δ*zwf1*), the first enzyme in the oxidative PPP, are auxotrophic for methionine as the high demand for NADPH in methionine biosynthesis cannot be met [46,47]. Lysine harvesting fully complemented the methionine auxotrophy of Δ*zwf1* cells, indicating a higher NADPH availability in lysine harvesting cells (Figure 3b). Next, we used a fluorescent, oxidant-dependent, NADPH sensor assay to directly measure the NADPH-mediated reducing power within cells upon H_2O_2 exposure. The fluorescent sensor confirmed increased NADPH availability in the lysine harvesters (Figure 3c and 3d).

A major destination for cellular NADPH flux is the glutathione pool, that under typical conditions, is maintained in a highly reduced equilibrium. Moreover, increased NADPH levels stimulate GSH levels, by increasing the activity of the first enzyme of the biosynthesis pathway, the gamma-glutamylcysteine ligase [48].We therefore constrained the FBA model in a second iteration, optimising the glutathione oxidoreductase reaction in which NADPH is consumed in order to convert oxidised glutathione into reduced

glutathione. With this change in constraint, the model predicted that lysine harvesting would enable the cells to increase the flux through the glutathione oxidoreductase reaction 7-fold, and furthermore, indicated that any excess lysine is diverted towards polyamine metabolism (Figure 3a, Supplementary Table 1 for the detailed list of reaction flux). To experimentally validate this result, we quantified the levels of reduced glutathione (GSH). Although GSH is one of the most abundant metabolites in WT cells, lysine harvesting promoted a further 7.85 fold increase in GSH concentration (Figure 3e).

The glutathione pool and the action of the glutathione oxidoreductase systems are the major components of the antioxidant defence mechanism. We therefore tested whether the boost in NADPH and glutathione levels driven by lysine harvesting would affect the resistance of *S. cerevisiae* to oxidants. First, we applied a thiol oxidising agent, diamide, to which resistance is known to increase with higher NADPH and GSH availability [11,12,49,50]. Lysine harvesting increased the resistance of the WT strain to diamide (Figure 3f). We compared this treatment to a methionine supplementation, about which we have previously shown to increase diamide resistance in a PPP-dependent manner [50]. Lysine harvesting provided a higher degree of resistance compared to methionine treatment (Figure 3f). Furthermore, we tested whether lysine harvesting would also protect against diamide when NADPH availability is scarce in Δ*zwf1* cells. Consistent with the hypothesis that antioxidant protection provided by lysine harvesting depends on increased NADPH availability, the protective effect was mitigated in unsupplemented Δ*zwf1* cells (Figure 3f). In parallel, we tested the response to H_2O_2. We grew WT cells in minimal media with and without lysine, in the presence of increasing concentrations of H_2O_2, and measured the resultant cell densities. Lysine harvesting substantially increased the resistance of WT cells to H_2O_2 compared to SM media (Figure 3g). Moreover, lysine harvesting cells had much lower intracellular ROS levels, even when exposed to high doses of the oxidant (10 mM H_2O_2), as revealed by dihydrorhodamine (DHR) staining (Figure 3h).

Several control experiments confirmed that the re-configuration of cellular metabolism, and not a direct antioxidant action of lysine, explain the protective effects. First, when we supplied D-lysine instead of L-lysine, which has identical redox properties but is biologically non-functional, cells became more sensitive to H_2O_2 (Figure 3g). Furthermore, pre-incubation of H_2O_2 with neither D- nor L-lysine did mitigate the cellular response to the oxidant, nor did lysine pre-incubation deplete H_2O_2 levels (Supplementary Figure 6). Additionally, we studied the effect of lysine on a panel of mammalian cell lines that are auxotrophic for lysine (HA1E, HeLa, A549 and BJhTERT). We confirmed that these also take up lysine (Supplementary Figure 7), but as native auxotrophs, cannot reconfigure their metabolism from lysine self-synthesis to uptake, and hence, cannot profit from re-channeling NADPH towards GSH biosynthesis. Indeed, there was no protective effect against H_2O_2 in any of the native auxotrophs (Supplementary Figure 8a). Complementarily, we tested whether the antioxidant effects of lysine harvesting are conserved among lysine prototrophs. Separated by billions of years of evolution, two non-

laboratory yeast strains isolated from palm wine in Cameroon and from a bakery in Korea, respectively (OS473 and OS265)[51] , the eukaryotes *Pichia pastoris, Candida tropicalis* (Supplementary Figure 8b and c), as well as the model bacterium *B. subtilis* (Supplementary Figure 8d), all gained resistance from lysine harvesting, demonstrating the conservation of this novel antioxidant strategy across several major clades of life.

DISCUSSION

We have shown that in the presence of physiological lysine concentrations, the amino acid is taken up in large quantities by cells from their environment, and that this uptake serves stress protection. In *Saccharomyces,* we detected intracellular lysine concentrations that are seventy to a hundred times above the concentrations measured in prototrophic cells under maximum growth rate in minimal media - the concentrations sufficient to achieve a maximum growth rate. Even assuming that part of the excessive intracellular lysine pool will be vacuolar, the activity of ornithine decarboxylase on lysine shows that cytoplasmic concentrations are also maintained in excess. Although Spe1p affinity for lysine is low (*Km* of > 3 mM), the enzyme forms high amounts of cadaverine. Mechanistically, a high accumulation is enabled by the transporter Lyp1p and its low affinity for intracellular lysine, leading to unidirectional transport [52], as well as the presence of the polyamine export machinery. Moreover, the harvesting strategy seems to be unique for lysine. Although the yeast cells switch effectively from self-synthesis to uptake for a panel of amino acids [53], the harvesting to extreme concentrations appears to be specific to only this amino acid (Figure 2b). Furthermore, the dependency on secondary metabolite processes (i.e. the polyamine pathway) indicated that metabolism is adapted to the harvesting of lysine. Indeed, for most metabolites cells do not tolerate an accumulation to such extreme levels; in part, as most metabolites become inhibitors to intrinsic enzymatic reactions if highly concentrated, and in part, as high metabolite concentrations stimulate unwanted promiscuous and non-enzymatic reactions [39,54].

Consistently, not only lysine, but also cadaverine was well tolerated and non-toxic for cells until extreme levels were induced by the over-expression of a bacterial lysine decarboxylase in lysine rich media - but equally - we could not find any direct advantage of intracellular or extracellular cadaverine. For instance, cadaverine was not directly protective against oxidants (H_2O_2, diamide, paraquat, cumene hydroperoxide), salts or starvation stress (Supplementary Note 1, 2 ,Supplementary Figure 11 and Table 2). Thus, we concluded that the high lysine levels itself must be the driving force behind the protective effect. Indeed, we found that high lysine concentrations protect the cells against oxidants, and were able to elucidate the molecular mechanism. Lysine harvesting decreases the metabolic competition for NADPH. Instead of reducing the flux through NADPH

forming reactions however, cells increase NADPH availability, and channel it into other metabolic processes, maintaining a much higher pool of reduced glutathione.

In summary, we have shown that in the presence of physiological nutrient concentrations, yeast cells specifically harvest large amounts of lysine. This harvest has at least two consequences (Figure 4). First, a promiscuous reaction of ornithine decarboxylase reaches relevant rates and forms an underground polyamine metabolite, cadaverine. The functionality of this alternative polyamine pathway is required for the cells to accumulate lysine to the extreme concentrations, and to maintain wild-type expression levels of the lysine biosynthetic enzymes. Second, the lysine harvest results in a metabolic re-configuration that enables cells to conserve more NADPH and maintain a much larger glutathione pool, to increase stress tolerance. Lysine harvesting hence adds to the series of mechanisms discovered over the last decade that involve supplementation of NADPH to prevent an imbalance in the redox state [11–13,15,55,56]. However, to our knowledge, none of the known mechanisms act quantitatively to induce an ~8-fold increase in the total glutathione pool prior to oxidant exposure. Hence, lysine harvesting may be one of the most powerful preventative and conditional metabolic antioxidant strategies available to microbial cells. Thus, microbial cells sense and take up metabolites from their environment not only to save energy and carbon equivalents for cell growth, but also to gain stress resistance and to increase robustness.

Acknowledgements

This work was supported by the Francis Crick Institute which receives its core funding from Cancer Research UK (FC001134), the UK Medical Research Council (FC001134), and the Wellcome Trust (FC001134), as well as received specific project funding from the Wellcome Trust (IA 200829/Z/16/Z to M.R.) and the ERC (StG 26809 to M.R.). We thank Consejo Nacional de Ciencia y Tecnología Mexico postdoctoral fellowship (232510 to V. O.-S.). We thank Alice Flint and Hassal Lee for assistance in the screening for a cadaverine function, and Dr. Andrew Carter and Dr. Edgar Morales-Rios from The Laboratory of Molecular Biology Medical Research Council (Cambridge) for providing their expertise in protein purification and allowing us to use their facilities.

Supplementary Note 1: Cadaverine formation is not toxic to yeast cells

We chose to increase cadaverine concentrations intracellularly by making use of metabolic engineering. We cloned a bacterial (*E. coli*) lysine decarboxylase (*ldc*C) and expressed it in the WT strain, BY4741. In SM, the expression of *ldcC* increased cadaverine concentrations 93.9 times (Supplementary Figure 9a). The expression of *ldcC* also affected the concentration of aminopropylcadaverine (APC), the cadaverine derived spermidine analogue, 5.5 times (Supplementary Figure 9b). In typical growth media, the modification and the increased intracellular concentration of the alternative polyamines had no effect on yeast growth (Supplementary Figure 9c). However, in lysine-rich media (250 μg/mL), the strain expressing *ldcC* exhibited a moderate growth defect (Supplementary Figure 9c). In this condition, cadaverine was elevated 192 times and APC 18.6 times above WT levels (Supplementary Figure 9a and 9b), concentrations that are unlikely to be reached under any physiological conditions in yeast. These results indicate that cadaverine and APC are well tolerated at the levels detected in cells and become only inhibitory to growth at extreme and non physiological concentrations.

Supplementary Note 2: Cadaverine can partially substitute for canonical polyamines, but only at non physiological high concentrations and certain pH

The putrescine-spermidine-spermine pathway is essential for yeast. The essentiality of Spe1p, Spe2p, Spe3p and Spe4p enzymes in SM can be rescued by adding their missing products (i.e. putrescine supplementation rescues a *SPE1* deletion, spermidine supplementation a *SPE1* and *SPE2* deletion, and so on [38,57,58]). To test whether cadaverine or aminopropylcadaverine (APC) complement the function of the canonical polyamines, we depleted the Δ*spe1* strain of external spermidine. Upon passaging in minimal polyamine-free media, the strain lost viability. Cadaverine could only rescue growth at very high and non physiological conditions (250 mM) (Supplementary Figure 10a). However, when Δ*spe1* strain was grown in the presence of 0.1 mM spermidine and 250 mM cadaverine, the growth rate of this strain improved compared to the one grown just in the presence of spermidine (Supplementary Figure 10b).

Eventually, we took advantage of the bacterial lysine decarboxylase LdcC to generate a strain that is incapable of producing the canonical polyamines putrescine, spermidine and spermidine but can form cadaverine and APC. This was achieved by deleting the ornithine decarboxylase *SPE1* and expressing *LdcC* (Δ*spe1 LdcC+*), in the presence of external spermidine, to prevent lethality. We inoculated the strain in minimal medium supplemented with lysine, to boost cadaverine production to high levels. The supplementation of lysine rescued Δ*spe1 LdcC+* strain, but fast growth rates were only obtained under acidic conditions, either in unbuffered synthetic minimal medium at a pH 5.0 or at 150 mM citrate/phosphate buffered minimal medium, also at pH 5.0. At neutral

or alkaline pH, complementation was minimal (Supplementary Figure 10c). One can derive two conclusions from these experiments. First, our experiments strongly suggest that the alternative polyamine pathway is not functioning as a substitute for the canonical polyamine pathway. The concentrations we had to generate, to achieve a complementation under some of the conditions are not seen in *Saccharomyces in vivo*. However, at the same time, the alternative polyamines have chemical properties that are not fundamentally different to that of the canonical polyamines either, because under specific conditions a partial complementation was achieved. As the alternative polyamine pathway does not work as a substitution for polyamine function, we were wondering if it has other properties important for the H_2O_2 response of cells. First, we tested whether cadaverine supplementation could simply have a direct protective effect for H_2O_2 treated cells or in other stress situations. We could not find a condition in which the external presence of cadaverine, or the expression of lysine decarboxylase, would have significantly altered survival in several stress-tolerance experiments (Supplementary Figure 11; Supplementary Table 2). Certainly, one can never test for all possible conditions, but as we could not find any protective effect in dozens of different stress tests conducted over several months, this is compelling evidence to indicate that it is not cadaverine that provides the antioxidant protection.

Materials and Methods

Yeast cultivation

Haploid wild-type (WT), Δ*lys2*, Δ*lys9*, Δ*lys12*, Δ*spe1*, Δ*spe2*, Δ*spe3,* Δ*spe4* strains of the S288c background (BY4741 and BY4742 derivatives [59]) transformed with the plasmid pHLUM (to repair auxotrophic markers [60]) were grown in synthetic minimal media (SM; 6.8 g/L yeast nitrogen base (Sigma-Aldrich)), supplemented with 2% glucose as carbon source. In Δ*zwf1 and* Δ*tpo1* strains of the *MAT*a yeast knockout collection we detected secondary mutations, and recreated the strains [50,61,62]. The Δ*spe1*-Δ*spe4* strains are auxotrophic for spermidine and thus cells were grown in the presence of 25 μg/mL lysine and 0.1 mM spermidine, respectively. WT and Δ*tpo1* cells were grown in SM with or without lysine or spermidine, as indicated. Δ*zwf1* was grown in SM supplemented with 40 μg/mL methionine or 100 μg/mL lysine. The *MAT*α WT strain of the S288c background BY4742 transformed with the plasmids pHLU or pHLUK, to repair auxotrophic markers [60], were grown in SM or synthetic complete media (SC; 0.56 g/L complete supplement mixture (MP Biomedicals) and 6.8 g/L yeast nitrogen base (Sigma-Aldrich)) supplemented with 2% glucose, with or without lysine.

Saccharomyces cerevisiae WT and Δ*zwf1* growth curves

WT and Δ*zwf1* cells were transferred from cryostock to solid SM media supplemented with 40 μg/mL methionine or 100 μg/mL lysine. Then 2 mL pre-cultures were grown in SM, SM + Met (colonies from SM + Met solid media) and SM + lysine (colonies from SM + lysine solid media), overnight at 30°C. The cultures were diluted to OD_{600nm} = 0.2 and incubated at 30°C. The growth was monitored in a multimode detector (Tecan Infinite 200 Pro) and OD_{600nm} was recorded until the cultures reached stationary phase. Data was analysed with the "grofit" R package [63] and illustrated using Origin Pro 9.0.

Hydrogen peroxide stress assays

Single WT colonies were picked and resuspended in 70 μL of SM. 20 μL of cell suspension was then transferred into the 3 conditions (SM, SM + L-Lys, SM + D-Lys, (L/D-Lys at 25 μg/mL)) and cultured overnight in a 3 ml culture volume at 30 ºC with shaking. The following day, this pre-culture was diluted to OD_{600nm} = 0.1 and 25 μL was used to inoculate 450 μL of respective media in a deep-well plate (450 μL media, 25 μL preculture, 25 μL H_2O_2) for a final OD_{600nm} of 0.005 and incubated for 16 h with H_2O_2 (0, 0.125, 0.25 and 0.5 mM). Resultant OD_{600nm} was measured to assess the tolerance of the cells to oxidant stress. For NADPH sensor experiments, wild-type auxotrophic yeast strains (BY4741 and BY4742) were transformed with a centromeric plasmid that permits constitutive expression of mKate2 in conjunction with Yap1p-ox dependent eGFP [64] selectable with *URA3* alone or in conjunction with the set of centromeric plasmids (pH, pL, pM or pK) that permits full

restoration of prototrophy. Following selection on SM + HLM/K or SM plates respectively, a single colony was picked and used to inoculate pre-cultures under the 3 conditions as above. Following exposure to H_2O_2, 200 µL of each culture was transferred to a 96-well plate and taken for high-throughput flow cytometry (BD Fortessa X20B/HTS). Median fluorescence intensity (MFI) was then obtained for both mKate2 and eGFP. mKate MFI values was then used to normalise eGFP values. Each condition was set up and analysed in quadruplicate.

Nutrient uptake rates

Nutrient uptake rates were determined as described previously [62]. *Saccharomyces cerevisiae* (BY4742) was transformed with the pHLU and pHLUK to compensate for auxotrophies including or excluding lysine [60], and were streaked on SM agar media with or without lysine supplementation, respectively. Then pre-cultures inoculated in SM or SM + Lys were grown overnight at 30ºC. The main cultures were initiated with an OD_{600nm} = 0.125 in 850 µL of SC or SM + Lys media in 96-well deep plates and incubated for 30h at 950 rpm and 30ºC with a 4 mm stirring bead per well. Then, 20 µL of cells were sampled every 3h and diluted 1:10 in water for OD_{600nm} measurement. Then, the cells were harvested at 3000 x*g* for 5 min and the supernatant was diluted 1:2 in absolute ethanol. 1 µL of the supernatant was used for quantification of extracellular lysine by LC/MS-MS.

Intracellular concentration of lysine in minimal media with or without lysine supplementation

Yeast cells were pre-cultured overnight in 50 mL of SM media with or without lysine (25 µg/mL) supplementation, and main cultures were initiated by diluting to an OD_{600nm} = 0.2-0.3 in 100 mL of SM media with or without lysine (25 µg/mL) supplementation. Cultures were grown until mid-log phase (OD_{600nm} approx 1.0) and samples for amino acid profile (1 ODU_{600nm}) were collected, washed with water and the pellet was frozen in dry ice. The samples were stored at -80°C.

Intracellular concentration of amino acids in yeast grown in different supplemented media

Strain BY4741 with auxotrophic loci repaired (HLUM knock-in) was woken up on YPD agar medium. Four colonies were picked and grown in 10 mL overnight SM pre-cultures. In a 96 deep-well plate, 1.4 mL cultures with a starting OD_{600nm} of 0.2, unsupplemented or supplemented with individual proteinogenic amino acids (except cysteine which inhibits growth and tyrosine which is hardly soluble) at a concentration of 0.334 mM or yeast extract (2%), were grown at 30°C for 6h with shaking. Samples were collected and processed as described in [43] with the exception that pellets were washed in 0.9 mL SM before lysis. Samples were analysed using multiple reaction monitoring on an Agilent 1290 liquid chromatography system coupled to an Agilent 6470 triple quadrupole mass

spectrometer using the acquisition and quantification by external calibration as described in [43].

ROS quantification by dihydrorhodamine staining

WT cells were grown in SM medium until mid-log phase. Then, cells were incubated with H_2O_2 (10 mM) for 1h. Subsequently, cells were harvested, washed 3 times in SM, and incubated for 90 minutes in the dark at 30ºC with 15 µM of dihydrorhodamine 123 (DHR 123). Cells were washed once with media and stained for 5 minutes with propidium iodide (500 µg/mL) to exclude dead cells, and subsequently washed 3 times with PBS. Cells were analysed by flow cytometry (BD LSRFortessa X20B/HTS) and quantification was done using FlowJo v9.6.2.

Identification of the candidate enzymes catalysing the biosynthesis of cadaverine

WT, Δ*spe1,* Δ*spe2,* Δ*spe3* and Δ*spe4* yeast were grown overnight in 10 mL of SM media with or without 0.1 mM spermidine, respectively, in the presence and absence of 25 µg/mL of lysine. Then, 10 ODU_{600nm} were collected and cadaverine was quantified by LC/MS-MS as outlined below (dansylation method). For the carbon tracing experiment, WT and Δ*spe1* were grown overnight in 100 mL of SM media with 0.1 mM spermidine. Then, [$^{13}C_6{}^{15}N_2$]-L-lysine was added to a final concentration of 0.12 mM and samples (10 ODU_{600nm}) were collected after 0 and 60 min. [$^{13}C_6{}^{15}N_2$]-cadaverine was quantified by LC/MS-MS as outlined below (dansylation method).

Gene amplification and cloning

Genomic DNA from *Saccharomyces cerevisiae* was isolated, and the *SPE1* coding sequence was amplified by PCR using primers CGTACCATGGATGTCTAGTACTCAAGTAGG (sense) and CATCCTCGAGATCGAGTTCAGAGTCTATG (antisense) introducing a *Nco*I and *Xho*I restriction site, respectively. The PCR product was cloned into the pGEM-T Easy vector (Promega) and *E. coli* DH5*α* were transformed with the plasmid. Plasmids were verified by sequencing. Then, the *SPE1* coding sequence was subcloned into the *Nco*I and *Xho*I sites of the pET20 plasmid (Novagen) in order to express a His-tagged protein.

Recombinant protein expression and purification

Escherichia coli BL21 was transformed with the plasmid for expression of *S. cerevisiae* 6xHIS-Spe1p. A 5 mL pre-culture was grown in Luria Bertani medium with 100 µg/mL ampicillin overnight at 37 °C. The next day, 10 mL of medium were inoculated with the overnight culture, cells grown until an OD_{600nm}= 0.6, and protein expression was induced with 1 mM isopropyl-b-D-thiogalactoside upon which the cells were grown for 4 h at 20°C. The cells were harvested and frozen at -80 °C. Then the frozen pellet was resuspended in

200 mL of lysis buffer (Tris-Cl 50 mM pH 7.4, NaCl 300 mM, 10 mM imidazole, 1 mM DTT, 1 tablet of EDTA-free protease inhibitors). The cells were lysed in a cell disruptor CF Range by passing the cell suspension three times at 30000 psi. The lysate was then ultra centrifuged at 185,511 x g at 4°C for 30 min. Spe1p was purified by IMAC on a HisTrap (Nickel) column (5 mL; GE Healthcare). The fractions with the peak of the protein of interest were combined and concentrated by centrifugation (2939 xg, 5 °C) through an Amicon Ultra-15 (molecular cut off 30 kDa, Millipore). The concentrated protein (500 µL) was injected to a Superdex S200 gel filtration column (10 x 300 mm; GE Healthcare) equilibrated with a buffer containing Tris-Cl 50 mM pH 7.4, NaCl 300 mM, 1 mM DTT and EDTA-free protease inhibitor tablets (1 tablet per 100 mL). The fractions with the purest Spe1p were identified by SDS-PAGE, combined and concentrated as mentioned above. 10% glycerol was added for preservation and the protein was stored at -80°C.

Kinetic characterisation of Spe1p

The activity of the recombinant Spe1p was determined by measuring the production of cadaverine or putrescine by LC/MS-MS. For measuring enzyme activities, the 0.25 mL standard reaction contained a mix of 40 mM HEPES pH 7.5, 8 mM ornithine, 0.1 mM EDTA, 1 mM DTT, 0.1 mM pyridoxal phosphate (PLP) and 0.1 mg/mL enzyme. The standard reaction for lysine decarboxylase activity was similar except for the addition of 20 mM lysine instead of ornithine. The *Km* for each substrate was determined by varying the concentrations of ornithine from 0-8 mM; or lysine from 0-20 mM. All kinetic parameters were recorded at 30°C. For determining enzyme activities, 30 µL of the reaction were sampled every minute and 120 µL of cold methanol was added to quench the reaction. Samples were kept on dry ice for 20 min and then centrifuged at high speed for 10 min. Supernatants were collected and putrescine and cadaverine were quantified by LC-MS/MS as outlined below.

Docking

The 3D structure of ornithine decarboxylase from *Saccharomyces cerevisiae* (Spe1p; UniProt ID: P08432 [41]) was obtained by homology modelling. The homology model was generated using Prime from Schrodinger suite (version 2015-3) and the structure of *Leishmania donovani* ornithine decarboxylases (PDB ID: 2OO0 [42]) as template. The cofactor (Vitamin B6 phosphate) and structural waters in the binding site were kept in the next steps. Ligand and protein structures were prepared using LigPrep and the Protein Preparation Wizard, respectively. Docking calculation was performed with Glide form Schrodinger Suite (version 2015-3) using GlideXP settings and the GlideScore version XP5.0 scoring function. Grid size used for calculation was 20 × 20 × 20 Å. The conformation with the best score was reported.

Modelling lysine uptake

In order to investigate the metabolic changes required to adapt for an excess of lysine in the media, a revised version of the *Saccharomyces cerevisiae* genome-scale metabolic model (iMM904_NADcorrected [45]) was used. In total 6 additional reactions related to cadaverine biosynthesis were added: two metabolic reactions for ornithine decarboxylase (h + lys_L --> co2 + cadaverine) and spermine synthase (S-adenosyl 3-(methylthio)propylamine + cadaverine --> S-methyl-5'-thioadenosine + aminopropylcadaverine), and four reactions were for transporting and exchanging cadaverine and aminopropylcadaverine to and from the cell. *In silico* SM constraints were used according to the original model (iMM904 [65]). For excess lysine uptake condition, in addition to the minimal media setting, the constraint of L-lysine exchange reaction (EX_lys_L(e)) was fixed to an arbitrarily large value 1, which is far more than the rate required for growth. The model simulations, using the flux balance analysis (FBA) approach, were performed in two steps. First, the maximum growth was predicted in the minimal media condition (we call it a naive model; Supplementary Figure 5). Then, the predicted growth rate was fixed and the rate of glutathione oxidoreductase reaction was maximised in both the minimal and lysine supplemented media conditions. COBRA toolbox [66] was used for all the model simulation.

Diamide resistance test

Cells were grown overnight in liquid minimal media with lysine (25 µg/mL) or methionine (40 µg/mL). The following day, the cultures were diluted to an OD_{600nm} = 1 in water, serial diluted (1:10) and spotted onto SM media containing either lysine (25 µg/mL) or methionine (40 µg/mL) and different concentrations of diamide (0-1.5 mM). Plates were incubated for 2-3 days.

Metabolite quantification

a. Amino acids

The amino acid extraction, separation and detection protocols were adapted from [43]. 100 µL 80% ethanol at 80°C was added to the frozen yeast pellet (1 ODU_{600nm}) from a mid-log phase culture, and the sample was incubated at 80°C for 2 min. Then, the sample was vortexed. The last two steps were repeated twice. The samples were centrifuged at 12000 x*g* for 5 min. The supernatants were collected and 1 µL was injected onto an analytical column (Waters ACQUITY UPLC BEH amide 1.7mm 2.1x100 mm) at 25°C. Buffer A consisted of 50:50 acetonitrile/water, 10 mM ammonium formate, 0.176% formic acid and buffer B was composed of 95:5:5 acetonitrile/methanol/water, 10 mM ammonium formate and 0.176% formic acid. The separation was performed at 0.9 mL/min isocratic flow with a gradient formed of the following steps: 0.7 min 85% Buffer B followed by a 1.85 min ramping to 5% B and keeping constant for 0.05 min before returning to the equilibrating

conditions of 85% B. The total running time was of 3.25 min. The quantification was carried out using a triple quadrupole mass spectrometer (Agilent 6460).

b. Quantification of polyamines

i) Dansylation derivatization method

Polyamines were quantified upon a derivatization with dansyl chloride (dansylation), following a protocol adapted from [67]. 200 mg of glass beads were added to the frozen cell pellets and were resuspended in 500 µL of 0.2 M $HClO_4$. Then, the cells were lysed in a homogenizer (FastPrep-24 5G MP Biomedicals) using 2 cycles of 20 seconds, 6.5 m/s at 4°C. The cell debris was removed by centrifugation at 12000 x *g* for 10 minutes at 4 °C and 100 µL were neutralised with 3 M sodium carbonate (10 µL). Then, 200 µL of 1,3-diaminopropane was added as an internal standard. The polyamines were dansylated by adding 400 µL of dansyl chloride in acetone (27 mM) to 100 µL of the sample and incubated at 60°C for 20 min in the dark. Then, 120 µL of a 0.8 M proline solution was added to the sample, vortexed and incubated at 25°C for 30 min in the dark. Then, an extraction with 500 µL of toluene was performed. The organic phase was taken and the solvent was removed under N_2 stream. Then, pellets were resuspended in 100 µL acetonitrile. 1 µL of the polyamines sample was separated using chromatography (Zorbax Eclipse Plus C18, RRHD, 2.1 x 50 mm, 1.8 µm) at 20°C. Buffer A consisted of 0.1% formic acid in water, and Buffer B was acetonitrile. The separation gradient consisted of an isocratic flow (0.5 mL/min) for 0.4 min of 60% B, followed by a ramp of 3.1 min to 100% B, then washing 0.3 min with 100% B then going back to starting conditions (60% B) in 0.01 min and 1.19 min for re-equilibration, resulting in a 5 min cycle time. The quantification was carried out using a Triple Quadrupole mass spectrometer (Agilent 6460).

ii) Non-derivatised method (for enzyme assays)

1 µL of the supernatant obtained from the kinetic assay was injected onto an analytical column (ACQUITY UPLC BEH amide 1.7 mm 2.1 x 100 mm), and putrescine and cadaverine were separated by HPLC. Buffer A consisted of 2:98 acetonitrile:water, 0.176% formic acid and Buffer B was composed of 95:5 acetonitrile:water, 0.176% formic acid. The separation gradient consisted of a 0.5 mL/min isocratic flow with the following steps: 0.25 min 100% Buffer B followed by a 0.25 min ramping to 72% B and keeping constant for 0.5 min. Then, a 1.5 min ramp to 30% B was done and kept constant for 0.5 min. A third 0.15 min ramp was done to 20% B and kept constant for 0.45 min before returning to the equilibrating conditions (100% B). The total running time was 5 min. The quantification was carried out using a Triple Quadrupole mass spectrometer (Agilent 6460).

c. GSH quantification

For GSH determination 5 ODU_{600nm} of mid-log phase WT cell cultures were harvested and quenched in one volume of 4 mM N-ethylmaleimide (NEM) in methanol previously cooled in dry ice [68]. The pellet was resuspended in 200 µL of a buffer composed by 75:25 (v/v) acetonitrile:methanol, 0.2% formic acid and lysed in a homogenizer (FastPrep-24 5G MP Biomedicals) using three cycles for 20 s at 6.5 m/s. Then, the sample was centrifuged for 5 min at 16000 x *g*. The pellet was extracted again with 200 µL of UHPLC water and both supernatants were combined and evaporated in a concentrator plus speedvac (Eppendorf), resuspended in 100 µL of 7% acetonitrile and centrifuged. 1 µL of the sample was injected onto a C8 column (ZORBAX SB-C8 Rapid Resolution HD, 2.1 x 100 mm, 1.8 µm (Agilent)) at 20°C. Buffer A was composed of 10% acetonitrile and Buffer B of 50% acetonitrile (v/v). Both buffers contained 750 mg/L octylammonium acetate as ion pairing reagent. The gradient consisted of 3.5 min of isocratic flow at 12% acetonitrile, followed by a 2.5 min gradient to 38% acetonitrile and a 0.5 min washing step to 42% acetonitrile and 1 min of re-equilibration to starting conditions with a total cycle time of 7.5 min. The quantification was carried out using a Triple Quadrupole mass spectrometer (Agilent 6470).

Proteomics data analysis

SWATH-MS data was previously reported [29], and is available via ProteomeXchange with identifier PXD013373. Raw data was analysed using Spectronaut Pulsar X software (Biognosys) with a previously reported spectral library (ProteomeXchange ID PXD013373). Protein quantities were calculated from all precursor intensities, and protein inference was performed using a protein database obtained from SGD (2018-08-28). Gene Ontology (GO) enrichment was performed in Spectronaut software using a gene annotation file obtained from SGD (2019-01-01). Data was analysed in R, with function "prcomp" for principal component analysis.

Statistical Analysis

The metabolite concentration data, the results from the growth curves analysis and the kinetic parameters are expressed as mean ± sd. The statistical significance was obtained using two sample Student's t test.

Table 1. Kinetic parameters of ornithine decarboxylase Spe1p

Substrate	*Km* (mM)	*Vm*/*Km* (mL*min^{-1}*mg^{-1})	Concentration (mM) SM	Concentration (mM) SM+lysine
Ornithine	0.0318 ± 0.006	88.9	2.04 ± 0.18 (WT) 1.6 ± 0.25 (*Δtpo1*)	2.2 ± 0.12 (WT) 2.2 ± 0.095 (*Δtpo1*)
Lysine	3.178 ± 1.5	0.095	3.02 ± 1.12 (WT) 2.45 ± 0.23 (*Δtpo1*)	215.2 ± 100.5 (WT) 104.2 ± 29.8 (*Δtpo1*)

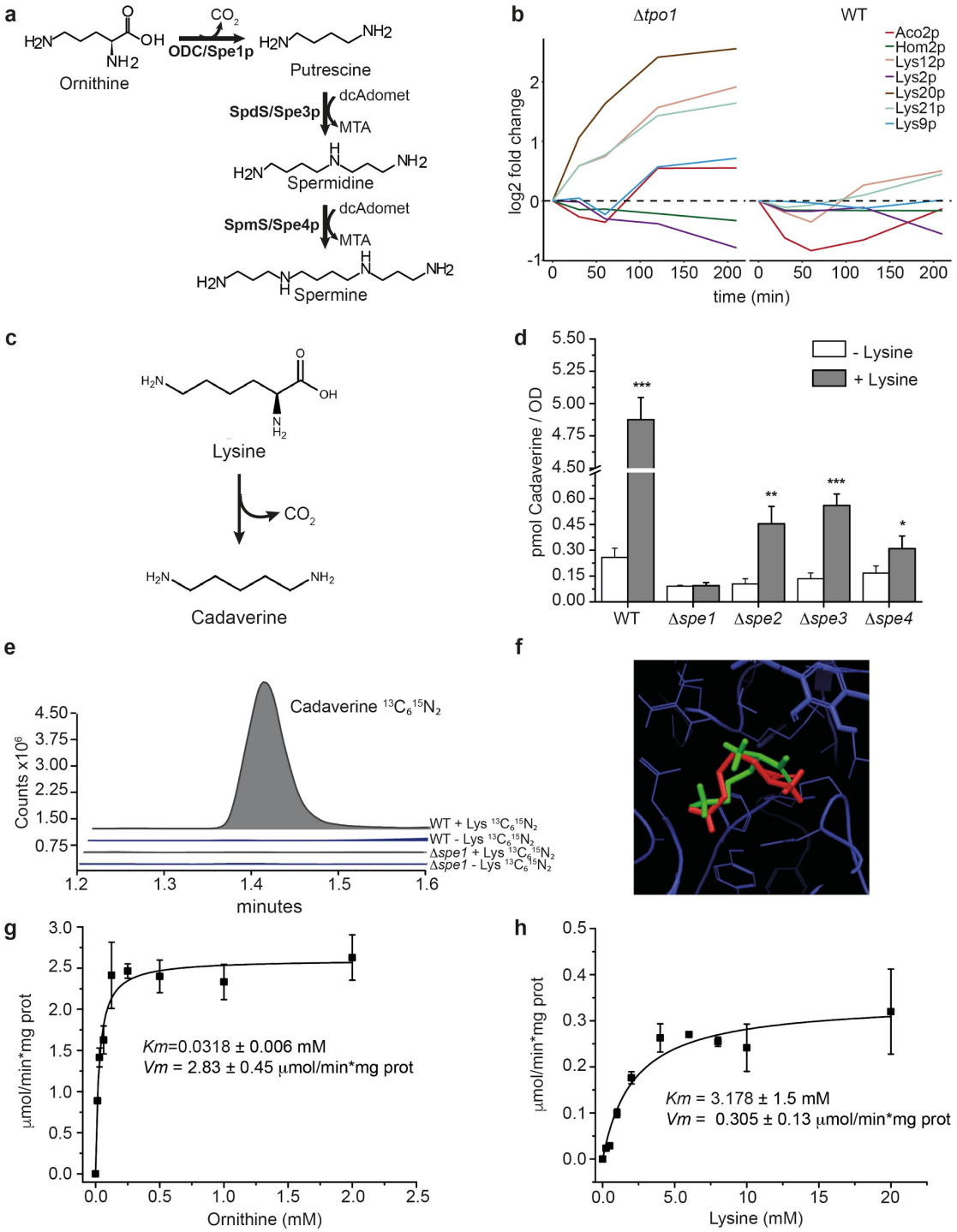
a
Ornithine
ODC/Spe1p
Putrescine
SpdS/Spe3p
dcAdomet
MTA
Spermidine
SpmS/Spe4p
Spermine
b
Δtpo1
WT
Aco2p
Hom2p
Lys12p
Lys2p
Lys20p
Lys21p
Lys9p
log2 fold change
time (min)
c
Lysine
Cadaverine
d
- Lysine
+ Lysine
pmol Cadaverine / OD
WT
Δspe1
Δspe2
Δspe3
Δspe4
e
Cadaverine $^{13}C_6{}^{15}N_2$
Counts x10^6
minutes
WT + Lys $^{13}C_6{}^{15}N_2$
WT - Lys $^{13}C_6{}^{15}N_2$
Δspe1 + Lys $^{13}C_6{}^{15}N_2$
Δspe1 - Lys $^{13}C_6{}^{15}N_2$
f
g
Km=0.0318 ± 0.006 mM
Vm = 2.83 ± 0.45 μmol/min*mg prot
μmol/min*mg prot
Ornithine (mM)
h
Km = 3.178 ± 1.5 mM
Vm = 0.305 ± 0.13 μmol/min*mg prot
μmol/min*mg prot
Lysine (mM)

Figure 1. A promiscuous reaction of Spe1p forms cadaverine from lysine in yeast
a. Schematic illustration of the canonical yeast polyamine biosynthesis pathway. Ornithine is decarboxylated to putrescine by Spe1p (ODC). Putrescine is then substrate of Spermidine Synthase (SpdS/Spe3p) that adds a methyl group to the diamine from the decarboxylated S-adenosylmethionine (dcAdoMet) forming spermidine and methylthioadenosine (MTA). Then spermine synthase (SpmS/Spe4p) adds a methyl group from dcAdoMet to spermidine forming spermine and methylthioadenosine (MTA). **b.** Several enzymes within the lysine biosynthetic pathway via aminoadipate are differentially expressed upon a H_2O_2 treatment, when the polyamine exporter *TPO1* is deleted. As described in [29], the cells were incubated 210 minutes with 1.5 mM H_2O_2 and analysed by SWATH-MS. The raw data (ProteomeXchange PXD013373) were re-processed with Spectronaut Pulsar X (Biognosys), and protein expression levels expressed as log2-fold change compared to untreated. **c.** Decarboxylation of lysine leads to the formation of cadaverine, a putrescine analogue. **d.** Cadaverine concentrations in overnight cultures of WT yeast and different knockouts of the polyamine biosynthesis pathway (*Δspe1-Δspe4*), in SM media supplemented or not with lysine (25 μg/mL). Bar charts represent the (mean ± sd, n = 3 or 4). Two sample Student's *t* test versus non supplemented condition: *p ≤ 0.05, **p ≤ 0.01, ***p ≤ 0.001. **e.** Chromatograms showing the $^{13}C_5{}^{15}N_2$ cadaverine formed after a 1 h incubation of WT and Δ*spe1* strains from isotope labelled lysine ($^{13}C_6{}^{15}N_2$ lysine). **f**. Results of docking lysine (red) and ornithine (green) to the same site of Spe1p using Glide from Schrodinger suite (version 2015-3) and an homology model based on the structure of *Leishmania donovani* ornithine decarboxylases (PDB ID: 2OO0 [42]). (**g**, **h**). *In vitro* activity of purified Spe1p on metabolizing ornithine (**g**) and lysine (**h**), respectively (mean ± sd, n = 3). The saturation curves were fitted to a Michaelis-Menten equation.

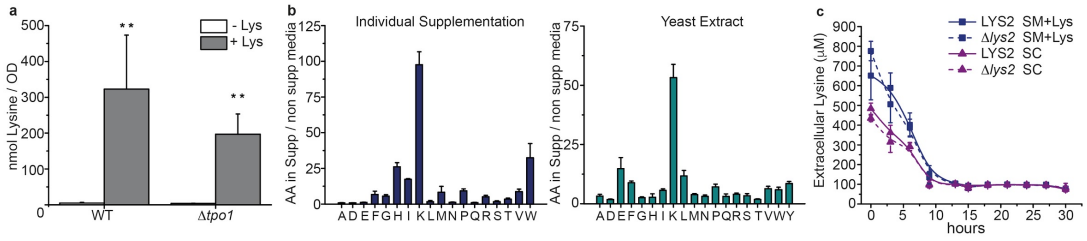

Figure 2. Lysine harvest in *Saccharomyces cerevisiae*. **a.** Lysine concentrations in WT and *Δtpo1* yeast grown in SM media supplemented or not with 25 μg/mL lysine. The cells were grown until mid-log phase and samples (1 $OD600_{nm}$ unit) were taken for amino acid determination by LC-MS/MS (mean ± sd, n = 3). Two sample Student's *t* test versus non supplemented condition: **p ≤ 0.01. **b.** Harvesting to reach extreme concentrations is specific for lysine. Strain BY4741 with repaired auxotrophic loci ("HLUM knock-in") was grown in SM media supplemented with individual amino acids or rich media (yeast extract) in quadruplicates. Cells were washed, intracellular amino acid profiles were measured and plotted above as fold-change (mean ± sd, n = 4) compared to the average profile of 7 replicates in unsupplemented SM media. **c.** Quantification of extracellular lysine of prototrophic and auxotrophic (Δ*lys2*) yeast grown in SC or SM media supplemented with lysine (SM+Lys). Cultures were initiated with an OD_{600nm} of 0.125 and let them grow for 30 h. Samples were taken every 3 h, harvested and the supernatant was used for quantification by LC/MS-MS. The data represent the mean ± sd, n = 4.

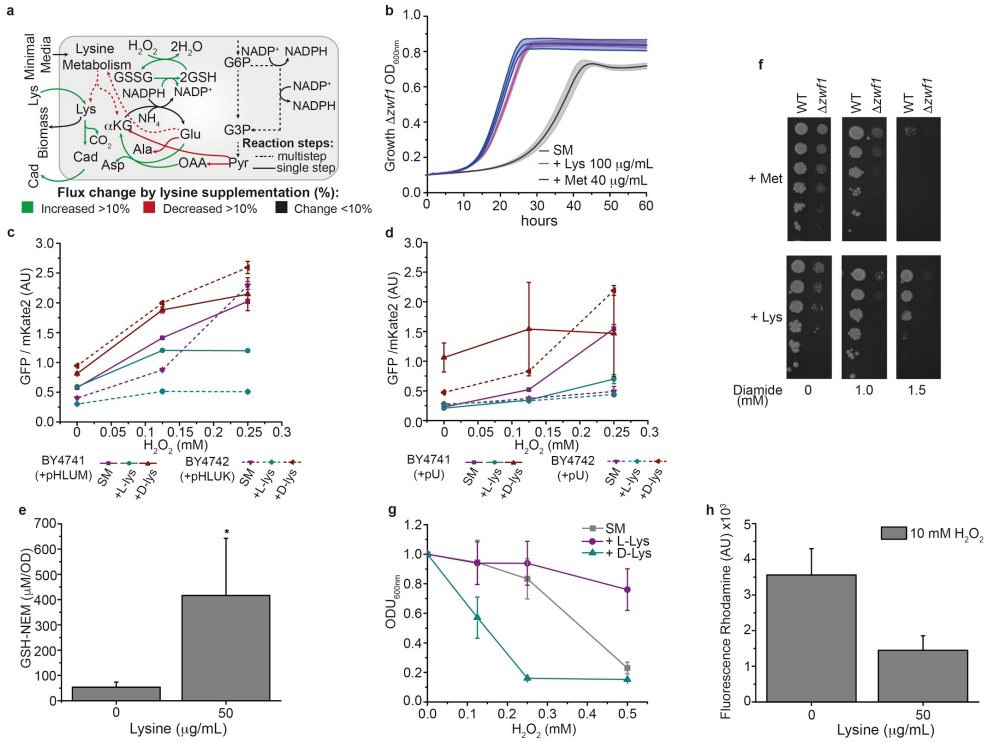

Figure 3. Lysine harvesting increases yeast antioxidant tolerances by replenishing NADPH and substantially increasing glutathione levels. a. Reprogramming of lysine metabolism replenishes the NADPH and GSH pool. Flux balance analysis of cells harvesting lysine in which growth rate was fixed and the rate of glutathione oxidoreductase reaction was maximised in both the minimal and lysine supplemented media conditions. **b.** Lysine harvesting complements the methionine auxotrophy of Δ*zwf1* yeast, that is caused by NADPH shortage. Growth curve showing Δ*zwf1* yeast grown in SM media supplemented or not with lysine (100μg/mL) or methionine (40μg/mL) (mean ± sd, n = 4). **c, d.** NADPH/NADP+ redox state estimated via a fluorescence biosensor assay in WT strains BY4741 and BY4742 ([64]), based on the principle that low NADPH levels induce GFP that is under the control of the TRX2 (cytoplasmic thioredoxin) promoter. GFP fluorescence signal was normalised to the fluorescence of constitutively expressed mKate2. **(c)** Strains transformed and fully complemented with pHLM+pU-sensor plasmids. **(d)** Strains supplemented with HLM amino acids and transformed with pU-sensor plasmid alone. The data represent the mean ± sd, n = 4. **e.** The pool of reduced glutathione (GSH) (measured as conjugate with N-ethylmaleimide) in WT yeast grown in SM media supplemented or not with lysine (50 μg/mL) data represents mean ± sd (n = 3). Two sample Student's *t* test versus non supplemented condition: $*p \leq 0.05$. **f.** Spot test showing the resistance of WT and Δ*zwf1* strain to diamide when grown in SM media supplemented with methionine (40 μg/mL) or lysine (25 μg/mL). Overnight cultures grown in SM media supplemented with lysine (25 μg/mL) or methionine (40 μg/mL) were diluted to an OD_{600nm} = 1 in water, serial diluted and spotted onto SM media containing either lysine or methionine and different concentrations of diamide (0-1.5 mM). **g.** L-lysine harvesting increases the H_2O_2 tolerance, but D-lysine has adverse effects. Cells were pre-cultured without lysine or in the presence of L-Lysine and D-Lysine and exposed to H_2O_2. Stress

tolerance was assessed by cell density measurement at OD_{600nm}. The data represent the mean ± sd, n = 4. **h.** ROS quantification by means of a dihydrorhodamine stain of WT cells incubated with 10 mM H_2O_2 for 1 h supplemented or not with lysine (50 μg/mL) (mean ± sd, n = 3).

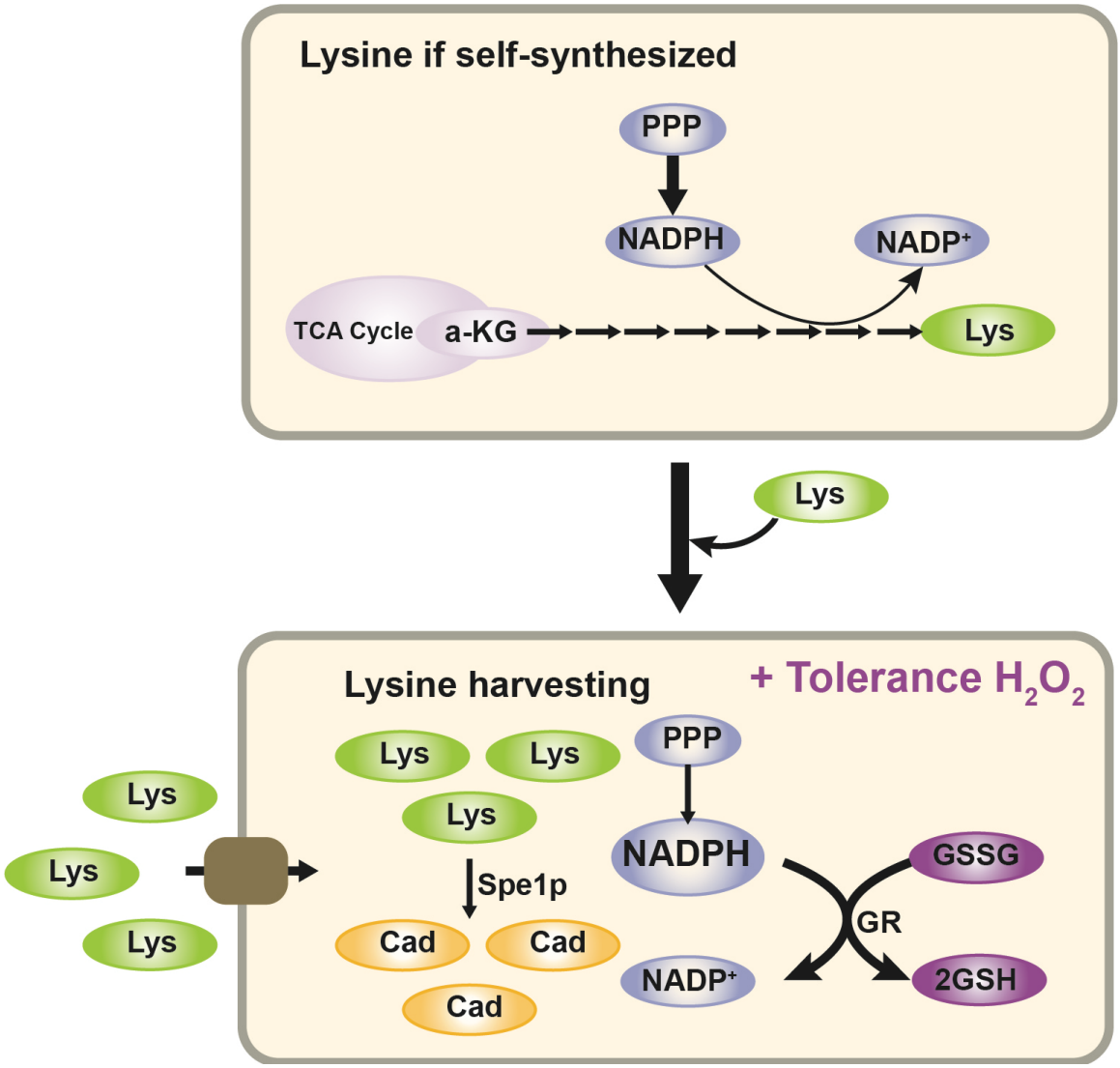

Figure 4. Schematic of proposed model by which lysine harvesting improves oxidant tolerance by reprogramming NADPH metabolism.

REFERENCES

1. Veal, E. A., Day, A. M. & Morgan, B. A. Hydrogen Peroxide Sensing and Signaling. *Mol. Cell* **26**, 1–14 (2007).
2. Morano, K. A., Grant, C. M. & Moye-Rowley, W. S. The response to heat shock and oxidative stress in Saccharomyces cerevisiae. *Genetics* **190**, 1157–1195 (2012).
3. Shackelford, R. E., Kaufmann, W. K. & Paules, R. S. Oxidative stress and cell cycle checkpoint function1. *Free Radical Biology and Medicine* **28**, 1387–1404 (2000).
4. McCord, J. M. & Fridovich, I. Superoxide dismutase. An enzymic function for erythrocuprein (hemocuprein). *J. Biol. Chem.* **244**, 6049–6055 (1969).
5. Carmel-Harel, O. & Storz, G. Roles of the glutathione- and thioredoxin-dependent reduction systems in the Escherichia coli and saccharomyces cerevisiae responses to oxidative stress. *Annu. Rev. Microbiol.* **54**, 439–461 (2000).
6. Thanan, R. *et al.* Oxidative stress and its significant roles in neurodegenerative diseases and cancer. *Int. J. Mol. Sci.* **16**, 193–217 (2014).
7. Pham-Huy, L. A., He, H. & Pham-Huy, C. Free radicals, antioxidants in disease and health. *Int. J. Biomed. Sci.* **4**, 89–96 (2008).
8. Li, J., O, W., Li, W., Jiang, Z.-G. & Ghanbari, H. A. Oxidative stress and neurodegenerative disorders. *Int. J. Mol. Sci.* **14**, 24438–24475 (2013).
9. Pollak, N., Dölle, C. & Ziegler, M. The power to reduce: pyridine nucleotides – small molecules with a multitude of functions. *Biochem. J* **402**, 205–218 (2007).
10. Holmgren, A. Antioxidant function of thioredoxin and glutaredoxin systems. *Antioxid. Redox Signal.* **2**, 811–820 (2000).
11. Ralser, M. *et al.* Dynamic rerouting of the carbohydrate flux is key to counteracting oxidative stress. *J. Biol.* **6**, 10 (2007).
12. Grüning, N.-M. *et al.* Pyruvate kinase triggers a metabolic feedback loop that controls redox

metabolism in respiring cells. *Cell Metab.* **14**, 415–427 (2011).

13. Anastasiou, D. *et al.* Inhibition of pyruvate kinase M2 by reactive oxygen species contributes to cellular antioxidant responses. *Science* **334**, 1278–1283 (2011).
14. Kuehne, A. *et al.* Acute Activation of Oxidative Pentose Phosphate Pathway as First-Line Response to Oxidative Stress in Human Skin Cells. *Mol. Cell* **59**, 359–371 (2015).
15. Christodoulou, D. *et al.* Reserve Flux Capacity in the Pentose Phosphate Pathway Enables Escherichia coli's Rapid Response to Oxidative Stress. *Cell Syst* **6**, 569–578.e7 (2018).
16. Ralser, M. *et al.* Metabolic reconfiguration precedes transcriptional regulation in the antioxidant response. *Nat. Biotechnol.* **27**, 604–605 (2009).
17. Gruning, N. M. N.-M. *et al.* Inhibition of triosephosphate isomerase by phosphoenolpyruvate in the feedback-regulation of glycolysis. *Open Biol.* **4**, 130232–130232 (2014).
18. Chechik, G. *et al.* Activity motifs reveal principles of timing in transcriptional control of the yeast metabolic network. *Nat. Biotechnol.* **26**, 1251–1259 (2008).
19. Peralta, D. *et al.* A proton relay enhances H2O2 sensitivity of GAPDH to facilitate metabolic adaptation. *Nat. Chem. Biol.* **11**, 156–163 (2015).
20. Miller-Fleming, L., Olin-Sandoval, V., Campbell, K. & Ralser, M. Remaining Mysteries of Molecular Biology: The Role of Polyamines in the Cell. *J. Mol. Biol.* **427**, 3389–3406 (2015).
21. Shah, P. & Swiatlo, E. A multifaceted role for polyamines in bacterial pathogens. *Mol. Microbiol.* **68**, 4–16 (2008).
22. Valdés-Santiago, L. & Ruiz-Herrera, J. Stress and polyamine metabolism in fungi. *Frontiers in chemistry* **1**, 42 (2013).
23. Rhee, H. J., Kim, E.-J. & Lee, J. K. Physiological polyamines: simple primordial stress molecules. *J. Cell. Mol. Med.* **11**, 685–703 (2007).
24. Pegg, A. E. Mammalian polyamine metabolism and function. *IUBMB Life* **61**, 880–894 (2009).

912 25. Kusano T. Berberich T. Tateda C., T. Y. Polyamines:essential factors for growth and
913 survival. *Planta* **228**, 367–381 (2008).
914 26. Igarashi, K. & Kashiwagi, K. Polyamines: mysterious modulators of cellular functions.
915 *Biochem. Biophys. Res. Commun.* **271**, 559–564 (2000).
916 27. Michael, A. J. Polyamines in Eukaryotes, Bacteria, and Archaea. *J. Biol. Chem.* **291**, 14896–
917 14903 (2016).
918 28. Løvaas, E. & Carlin, G. Spermine: an anti-oxidant and anti-inflammatory agent. *Free Radic.*
919 *Biol. Med.* **11**, 455–461 (1991).
920 29. Krüger, A. *et al.* Tpo1-mediated spermine and spermidine export controls cell cycle delay
921 and times antioxidant protein expression during the oxidative stress response. *EMBO Rep.*
922 (2013). doi:10.1038/embor.2013.165
923 30. Mima, S. *et al.* Identification of the TPO1 gene in yeast, and its human orthologue
924 TETRAN, which cause resistance to NSAIDs. *FEBS Lett.* **581**, 1457–1463 (2007).
925 31. Albertsen, M., Bellahn, I., Kramer, R. & Waffenschmidt, S. Localization and function of the
926 yeast multidrug transporter Tpo1p. *J. Biol. Chem.* **278**, 12820–12825 (2003).
927 32. Uemura, T., Tachihara, K., Tomitori, H., Kashiwagi, K. & Igarashi, K. Characteristics of the
928 polyamine transporter TPO1 and regulation of its activity and cellular localization by
929 phosphorylation. *J. Biol. Chem.* **280**, 9646–9652 (2005).
930 33. Gillet, L. C. *et al.* Targeted data extraction of the MS/MS spectra generated by data-
931 independent acquisition: a new concept for consistent and accurate proteome analysis. *Mol.*
932 *Cell. Proteomics* **11**, O111.016717 (2012).
933 34. Zelezniak, A. *et al.* Machine Learning Predicts the Yeast Metabolome from the Quantitative
934 Proteome of Kinase Knockouts. *Cell Syst* **7**, 269–283.e6 (2018).
935 35. Tomar, P. C., Lakra, N. & Mishra, S. N. A lysine catabolite involved in plant growth and
936 development Cadaverine. 1–15 (2013).
937 36. Yamamoto, Y., Miwa, Y., Miyoshi, K., Furuyama, J. & Ohmori, H. The Escherichia coli

938 ldcC gene encodes another lysine decarboxylase, probably a constitutive enzyme. *Genes*
939 *Genet. Syst.* **72**, 167–172 (1997).
940 37. Igarashi, K. *et al.* Formation of a compensatory polyamine by Escherichia coli polyamine-
941 requiring mutants during growth in the absence of polyamines. *J. Bacteriol.* **166**, 128–134
942 (1986).
943 38. Whitney, P. A. & Morris, D. R. Polyamine auxotrophs of Saccharomyces cerevisiae. *J.*
944 *Bacteriol.* **134**, 214–220 (1978).
945 39. Keller, M. A., Piedrafita, G. & Ralser, M. The widespread role of non-enzymatic reactions in
946 cellular metabolism. *Curr. Opin. Biotechnol.* **34**, 153–161 (2015).
947 40. Taxis, C. A safety catch for ornithine decarboxylase degradation. *Microb. Cell Fact.* **2**, 174–
948 177 (2015).
949 41. Tyagi, A. K., Tabor, C. W. & Tabor, H. Ornithine decarboxylase from Saccharomyces
950 cerevisiae. Purification, properties, and regulation of activity. *J. Biol. Chem.* **256**, 12156–
951 12163 (1981).
952 42. Dufe, V. T. *et al.* A structural insight into the inhibition of human and Leishmania donovani
953 ornithine decarboxylases by 1-amino-oxy-3-aminopropane. *Biochem. J* **405**, 261–268
954 (2007).
955 43. Mülleder, M. *et al.* Functional Metabolomics Describes the Yeast Biosynthetic Regulome.
956 *Cell* **167**, 553–565.e12 (2016).
957 44. Cornish-Bowden, A. *Principles of Enzyme Kinetics*. (Elsevier, 2014).
958 45. Szappanos, B. *et al.* An integrated approach to characterize genetic interaction networks in
959 yeast metabolism. *Nat. Genet.* **43**, 656–662 (2011).
960 46. Nogae, I. & Johnston, M. Isolation and characterization of the ZWF1 gene of
961 Saccharomyces cerevisiae, encoding glucose-6-phosphate dehydrogenase. *Gene* **96**, 161–169
962 (1990).
963 47. Slekar, K. H., Kosman, D. J. & Culotta, V. C. The yeast copper/zinc superoxide dismutase

964 and the pentose phosphate pathway play overlapping roles in oxidative stress protection. *J.*
965 *Biol. Chem.* **271**, 28831–28836 (1996).
966 48. Toroser, D., Yarian, C. S., Orr, W. C. & Sohal, R. S. Mechanisms of γ-glutamylcysteine
967 ligase regulation. *Biochimica et Biophysica Acta (BBA) - General Subjects* **1760**, 233–244
968 (2006).
969 49. Shenton, D. & Grant, C. M. Protein S-thiolation targets glycolysis and protein synthesis in
970 response to oxidative stress in the yeast Saccharomyces cerevisiae. *Biochem. J* **374**, 513–519
971 (2003).
972 50. Campbell, K., Vowinckel, J., Keller, M. A. & Ralser, M. Methionine Metabolism Alters
973 Oxidative Stress Resistance via the Pentose Phosphate Pathway. *Antioxid. Redox Signal.* **14**,
974 1–14 (2016).
975 51. Peter, J. *et al.* Genome evolution across 1,011 Saccharomyces cerevisiae isolates. *Nature*
976 **556**, 339–344 (2018).
977 52. Bianchi, F. *et al.* Asymmetry in inward- and outward-affinity constant of transport explain
978 unidirectional lysine flux in Saccharomyces cerevisiae. *Sci. Rep.* **6**, 31443 (2016).
979 53. Alam, M. T. *et al.* The metabolic background is a global player in Saccharomyces gene
980 expression epistasis. *Nat Microbiol* **1**, 15030 (2016).
981 54. Alam, M. T. *et al.* The self-inhibitory nature of metabolic networks and its alleviation
982 through compartmentalization. *Nat. Commun.* **8**, 16018 (2017).
983 55. Rajasekaran, N. S. *et al.* Human alpha B-crystallin mutation causes oxido-reductive stress
984 and protein aggregation cardiomyopathy in mice. *Cell* **130**, 427–439 (2007).
985 56. Cosentino, C., Grieco, D. & Costanzo, V. ATM activates the pentose phosphate pathway
986 promoting anti-oxidant defence and DNA repair. *EMBO J.* **30**, 546–555 (2011).
987 57. Hamasaki-Katagiri, N., Tabor, C. W. & Tabor, H. Spermidine biosynthesis in
988 Saccharomyces cerevisiae: Polyaminerequirement of a null mutant of the SPE3 gene
989 (spermidine synthase). *Gene* **187**, 35–43 (1997).

58. Hamasaki-Katagiri, N., Katagiri, Y., Tabor, C. W. & Tabor, H. Spermine is not essential for growth of Saccharomyces cerevisiae: identification of the SPE4 gene (spermine synthase) and characterization of a spe4 deletion mutant. *Gene* **210**, 195–201 (1998).

59. Brachmann, C. B. *et al.* Designer deletion strains derived from Saccharomyces cerevisiae S288C: a useful set of strains and plasmids for PCR-mediated gene disruption and other applications. *Yeast* **14**, 115–132 (1998).

60. Mülleder, M., Campbell, K., Matsarskaia, O., Eckerstorfer, F. & Ralser, M. Saccharomyces cerevisiae single-copy plasmids for auxotrophy compensation, multiple marker selection, and for designing metabolically cooperating communities. *F1000Res.* **5**, 2351 (2016).

61. Ralser, M. *et al.* A catabolic block does not sufficiently explain how 2-deoxy-D-glucose inhibits cell growth. *Proc. Natl. Acad. Sci. U. S. A.* **105**, 17807–17811 (2008).

62. Campbell, K. *et al.* Self-establishing communities enable cooperative metabolite exchange in a eukaryote. *Elife* **4**, (2015).

63. Kahm, M. *et al.* grofit: fitting biological growth curves with R. *J. Stat. Softw.* **33**, 1–21 (2010).

64. Zhang, J. *et al.* Engineering an NADPH/NADP Redox Biosensor in Yeast. *ACS Synthetic Biology* **5**, 1546–1556 (2016).

65. Mo, M. L., Palsson, B. O. & Herrgård, M. J. Connecting extracellular metabolomic measurements to intracellular flux states in yeast. *BMC Syst. Biol.* **3**, 37 (2009).

66. Heirendt, L. *et al.* Creation and analysis of biochemical constraint-based models: the COBRA Toolbox v3.0. *arXiv [q-bio.QM]* (2017).

67. Reyes-Becerril, M., Esteban, M. Á., Tovar-Ramírez, D. & Ascencio-Valle, F. Polyamine determination in different strains of the yeast Debaryomyces hansenii by high pressure liquid chromatography. *Food Chem.* **127**, 1862–1865 (2011).

68. Sasidharan, K., Soga, T., Tomita, M. & Murray, D. B. A yeast metabolite extraction protocol optimised for time-series analyses. *PLoS One* **7**, e44283 (2012).

1016